Toll-like receptor 4–induced ryanodine receptor 2 oxidation and sarcoplasmic reticulum Ca^{2+} leakage promote cardiac contractile dysfunction in sepsis

Received for publication, August 22, 2017, and in revised form, November 3, 2017 Published, Papers in Press, November 17, 2017, DOI 10.1074/jbc.M117.812289

Jie Yang[‡§1], Rui Zhang[‡1], Xin Jiang[¶1], Jingzhang Lv[‖], Ying Li[§], Hongyu Ye[**], Wenjuan Liu[§], Gang Wang[§], Cuicui Zhang[§], Na Zheng[§], Ming Dong[§], Yan Wang[§], Peiya Chen[§], Kumar Santosh[§], Yong Jiang[‡2], and Jie Liu[‡§3]

From the [‡]Department of Pathophysiology, Southern Medical University, Guangzhou 510515, China, the [§]Department of Pathophysiology, School of Medicine, Shenzhen University, Shenzhen 518060, China, the [¶]Department of Cardiology, Second Affiliated Hospital of Jinan University (Shenzhen People's Hospital), Shenzhen 518000, China, the [‖]Shenzhen Entry-Exit Inspection and Quarantine Bureau, Shenzhen 518045, China, and the [**]Department of Cardiothoracic Surgery, Zhongshan People's Hospital, Zhongshan 528415, China

Edited by Roger J. Colbran

Studies suggest the potential role of a sarcoplasmic reticulum (SR) Ca^{2+} leak in cardiac contractile dysfunction in sepsis. However, direct supporting evidence is lacking, and the mechanisms underlying this SR leak are poorly understood. Here, we investigated the changes in cardiac Ca^{2+} handling and contraction in LPS-treated rat cardiomyocytes and a mouse model of polymicrobial sepsis produced by cecal ligation and puncture (CLP). LPS decreased the systolic Ca^{2+} transient and myocyte contraction as well as SR Ca^{2+} content. Meanwhile, LPS increased Ca^{2+} spark–mediated SR Ca^{2+} leak. Preventing the SR leak with ryanodine receptor (RyR) blocker tetracaine restored SR load and increased myocyte contraction. Similar alterations in Ca^{2+} handling were observed in cardiomyocytes from CLP mice. Treatment with JTV-519, an anti-SR leak drug, restored Ca^{2+} handling and improved cardiac function. In the LPS-treated cardiomyocytes, mitochondrial reactive oxygen species and oxidative stress in RyR2 were increased, whereas the levels of the RyR2-associated FK506-binding protein 1B (FKBP12.6) were decreased. The Toll-like receptor 4 (TLR4)–specific inhibitor TAK-242 reduced the oxidative stress in LPS-treated cells, decreased the SR leak, and normalized Ca^{2+} handling and myocyte contraction. Consistently, TLR4 deletion significantly improved cardiac function and corrected abnormal Ca^{2+} handling in the CLP mice. This study provides evidence for the critical role of the SR Ca^{2+} leak in the development of septic cardiomyopathy and highlights the therapeutic potential of JTV-519 by preventing SR leak. Furthermore, it reveals that TLR4 activation-induced mitochondrial reactive oxygen species production and the resulting oxidative stress in RyR2 contribute to the SR Ca^{2+} leak.

Sepsis is the most common cause of mortality in intensive care units, and the incidence is increasing (1). Myocardial dysfunction is a recognized manifestation of sepsis, which occurs in 40% of patients diagnosed with sepsis and dramatically increases mortality from 20% to as high as 70–90% (2). The most common defect in cardiac performance during sepsis is impaired contractility of the ventricles (3). Evidence suggests that dysregulation of myocardial Ca^{2+} handling accounts for the reduced contractile force in septic cardiomyopathy (4, 5). The abnormalities in Ca^{2+} regulation have been suggested to occur at practically all main steps of Ca^{2+} handling, including decreased sarcolemmal Ca^{2+} entry through L-type Ca^{2+} channels, impaired sarcoplasmic reticulum (SR)[4] Ca^{2+} release and recycling, and reduced myofibrillar Ca^{2+} sensitivity, although some results are conflicting (6, 7).

In the mammalian heart, the major source of Ca^{2+} required for contractile activation is the SR (8). During cardiac EC coupling, depolarization activates Ca^{2+} entry through L-type Ca^{2+} channels in the sarcolemmal membrane, triggering a large amount of Ca^{2+} release from SR via ryanodine receptors (RyRs) through a Ca^{2+}-induced Ca^{2+} release mechanism (4, 9). The simultaneous systolic SR Ca^{2+} release gives rise to a global intracellular Ca^{2+} transient, which consequently initiates myofilament contraction. In septic cardiomyopathy, the systolic Ca^{2+} transient is decreased, which is associated with a decrease in the SR Ca^{2+} content (4, 10, 11). It is well established that the SR Ca^{2+} content is finely tuned by the SR Ca^{2+} recycling

This work was supported by National Science Foundation of China Grants 31371159 and 31671179 (to J. L.), 81401570 (to J. X.), 31400982 (to W. L.), 81670211 (to G. W.), and 81372030 (to J. Y.); by Basic Research Foundation of SZ Grant JCYJ20160308091147262 (to J. L.); by NSFC-Guangdong Joint Foundation of China Grant U1601225 (to J. Y.); and by Key Scientific and Technological Program of Guangzhou City Grant 201607020016 (to J. Y.). The authors declare that they have no conflicts of interest with the contents of this article.

This article contains Figs. S1 and S2.

[1] These authors contributed equally to this work.

[2] To whom correspondence may be addressed: Guangdong Provincial Key Laboratory of Proteomics, State Key Laboratory of Organ Failure Research, Southern Medical University, Guangzhou 510515, China. Tel./Fax: 86-20-61648231; E-mail: jiang48231@163.com.

[3] To whom correspondence may be addressed: Dept. of Pathophysiology, School of Medicine, Shenzhen University, Shenzhen 518060, China. Tel./Fax: 86-755-86671906; E-mail: liuj@szu.edu.cn.

[4] The abbreviations used are: SR, sarcoplasmic reticulum; RyR, ryanodine receptor; ROS, reactive oxygen species; CLP, cecal ligation and puncture; LV, left ventricular; FS, fractional shortening; mBB, monobromobimane; ROS, reactive oxygen species; mitoROS, mitochondrial ROS; MitoSOX, 5-(and-6)-chloromethyl 2′,7′- dichlorodihydrofluorescein diacetate; mito-TEMPO, (2-(2,2,6,6-tetramethylpiperidin-1-oxyl-4-ylamino)-2-oxoethyl)triphenylphosphonium chloride; EF, ejection fraction; LVIDd and LVIDs, LV internal dimensions at diastole and systole, respectively.

through SR Ca^{2+}-ATPase and diastolic SR Ca^{2+} release, also called SR Ca^{2+} leak, through the RyRs (9, 12). In a number of reports, the reduced SR Ca^{2+} content has been attributed to the depressed SR Ca^{2+}-ATPase function (12–14). Another potential cause of the reduced SR Ca^{2+} content is increased diastolic SR Ca^{2+} leak. Zhu *et al.* (15) demonstrated that increased Ca^{2+} spark frequency and diminished SR Ca^{2+} content were simultaneously present in cardiomyocytes from septic rats. Although enhanced Ca^{2+} spark–mediated SR Ca^{2+} leak may explain the reduced SR Ca^{2+} content, direct experimental support for the causal relationship is lacking. Particularly, the underlying mechanism for the increased SR Ca^{2+} leak in septic cardiomyopathy remains poorly understood.

It is well established that excessive inflammatory response and intracellular oxidative stress play important roles in the development of septic cardiomyopathy (16). The cross-talk between inflammation and reactive oxidative species (ROS) further promotes intracellular oxidative stress. In heart failure and burn-generated cardiac dysfunction, the enhancement of intracellular oxidative stress has been suggested to cause SR Ca^{2+} leak by increasing diastolic RyR activity (17–19). In sepsis, the activation of the Toll-like receptor 4 (TLR4) signaling pathways stimulates inflammatory and oxidative responses, leading to the development of septic cardiomyopathy (20, 21). However, it remains unknown whether TLR4 mediates cardiac dysfunction through inducing SR Ca^{2+} leak in sepsis.

Therefore, in this study, we studied the possible contribution of TLR4 signaling to the abnormal SR function and cardiac dysfunction in sepsis by using an LPS-induced cell model of sepsis and a cecal ligation and puncture (CLP)–induced mouse model of polymicrobial sepsis. Furthermore, we explored the potential therapeutic effect of JTV-519, a newly developed drug with the activity of preventing SR Ca^{2+} leak, possibly by stabilizing RyR channels, on treatment of septic cardiomyopathy.

Results

LPS decreases intracellular Ca^{2+} transient and cardiac contractility by reducing SR Ca^{2+} content

We first examined the effect of LPS on intracellular Ca^{2+} transient and cell shortening in cardiomyocytes paced with 1-Hz field stimulation. The results show that LPS treatment for 30 min significantly decreased Ca^{2+} transient and cell shortening in a dose-dependent manner. The amplitude of Ca^{2+} transient was decreased by 10.8, 26.9, and 34.2% by 250, 500, and 1000 ng/ml LPS, respectively (Fig. 1, *A* and *B*). Consistently, the cardiac contractility was remarkably decreased by LPS treatment in a dose-dependent manner, where the cell shortening was decreased by 8.1, 17.8, and 36.7% by 250, 500, and 1000 ng/ml LPS, respectively (Fig. 1*C*). Furthermore, LPS slowed the kinetics of Ca^{2+} transient, where the half-time of decay of the Ca^{2+} transient (T_{50}) was increased by LPS treatment (Fig. 1*D*).

It is known that SR is the major source for intracellular Ca^{2+} transient, and the reduction in SR load results in a decrease of the Ca^{2+} transient (9). We thus explored whether the reduction in systolic Ca^{2+} transient is related to the alteration of SR Ca^{2+} content. In parallel to the decrease of Ca^{2+} transient, LPS reduced SR Ca^{2+} content in a dose-dependent manner (Fig. 1, *E* and *F*). The amplitude of caffeine-induced Ca^{2+} transient, which reflects SR load, was decreased by 22.1, 36.2, and 45.5% by 250, 500, and 1000 ng/ml LPS, respectively (Fig. 1*F*). The results suggest that LPS decreases systolic Ca^{2+} transient and cardiac contractility through reducing SR Ca^{2+} content. The half-time of decay (T_{50}) of the Ca^{2+} transient was not significantly changed (Fig. 1*G*), suggesting that LPS had no effect on the activity of Na^{+}-Ca^{2+} exchanger.

Increased Ca^{2+} spark–mediated SR leak contributes to the reduction of SR load in LPS-treated cardiomyocytes

We next explored the possible contribution of SR Ca^{2+} leak to the reduction of SR Ca^{2+} content. Observing diastolic Ca^{2+} spark provides a window visualizing the resting RyR Ca^{2+} release (or Ca^{2+} leak) and SR function. We found that LPS dose-dependently increased the occurrence of Ca^{2+} spark. The frequency of Ca^{2+} sparks was increased by 51.1, 81.8, and 120% by 250, 500, and 1000 ng/ml LPS, respectively (Fig. 2, *A* and *B*). Meanwhile, the amplitude of Ca^{2+} sparks was decreased (Fig. 2*C*), which is consistent to the reduction of SR Ca^{2+} content. LPS had no significant effect on the size (full width of half-maximum, *FWHM*) (Fig. 2*D*) and kinetics (full duration of half-maximum, *FDHM*) of the Ca^{2+} sparks (Fig. 2*E*).

To probe the causal relationship between Ca^{2+} spark–mediated Ca^{2+} leak and the reduction of SR Ca^{2+} content upon LPS stimulation, we used RyR blocker, tetracaine, to inhibit Ca^{2+} spark–mediated SR Ca^{2+} leak and investigated the effect on the SR Ca^{2+} load. Previous studies have demonstrated that tetracaine dose-dependently regulates Ca^{2+} handling and myocyte contractility. The study by Venetucci *et al.* (22) showed that tetracaine at lower concentration (20–50 μM) had no significant effect on the amplitude of Ca^{2+} transient in isoproterenol-treated cardiomyocytes with no diastolic release but increased Ca^{2+} transient amplitude in the cells preceded by diastolic release (22). Our previous study had also shown that tetracaine at 50 μM prevented the increased diastolic SR Ca^{2+} leak without affecting normal Ca^{2+} handling (20). We thus pretreated the cells with 50 μM tetracaine for 30 min before LPS stimulation. Tetracaine significantly decreased Ca^{2+} spark frequency (Fig. 3*A*) and largely restored the reduced SR load (Fig. 3*B*) in LPS-treated cells, indicating that SR leak is an important reason for the diminished SR load. Furthermore, the peak systolic Ca^{2+} transient and cell shortening were significantly increased with the restoration of SR load (Fig. 3, *C* and *D*), confirming the notion that LPS decreased myocyte contractility by partially depleting SR Ca^{2+} content.

Prevention of SR Ca^{2+} leak with JTV-519 improves cardiac function in septic mice

A mouse model of polymicrobial sepsis was produced by CLP. Cardiac function was monitored with echocardiography 6 h after the surgery (23–25). Consistent with a previous report, the cardiac function in septic mice was impaired as compared with control, where the left ventricular (LV) functions indexed by the fractional shortening (FS) and ejection fraction (EF) were remarkably decreased (Fig. 4, *A*–*C*). The Ca^{2+} handling and myocyte contraction were examined in cardiomyocytes isolated from the hearts of control (sham) or septic mice. The

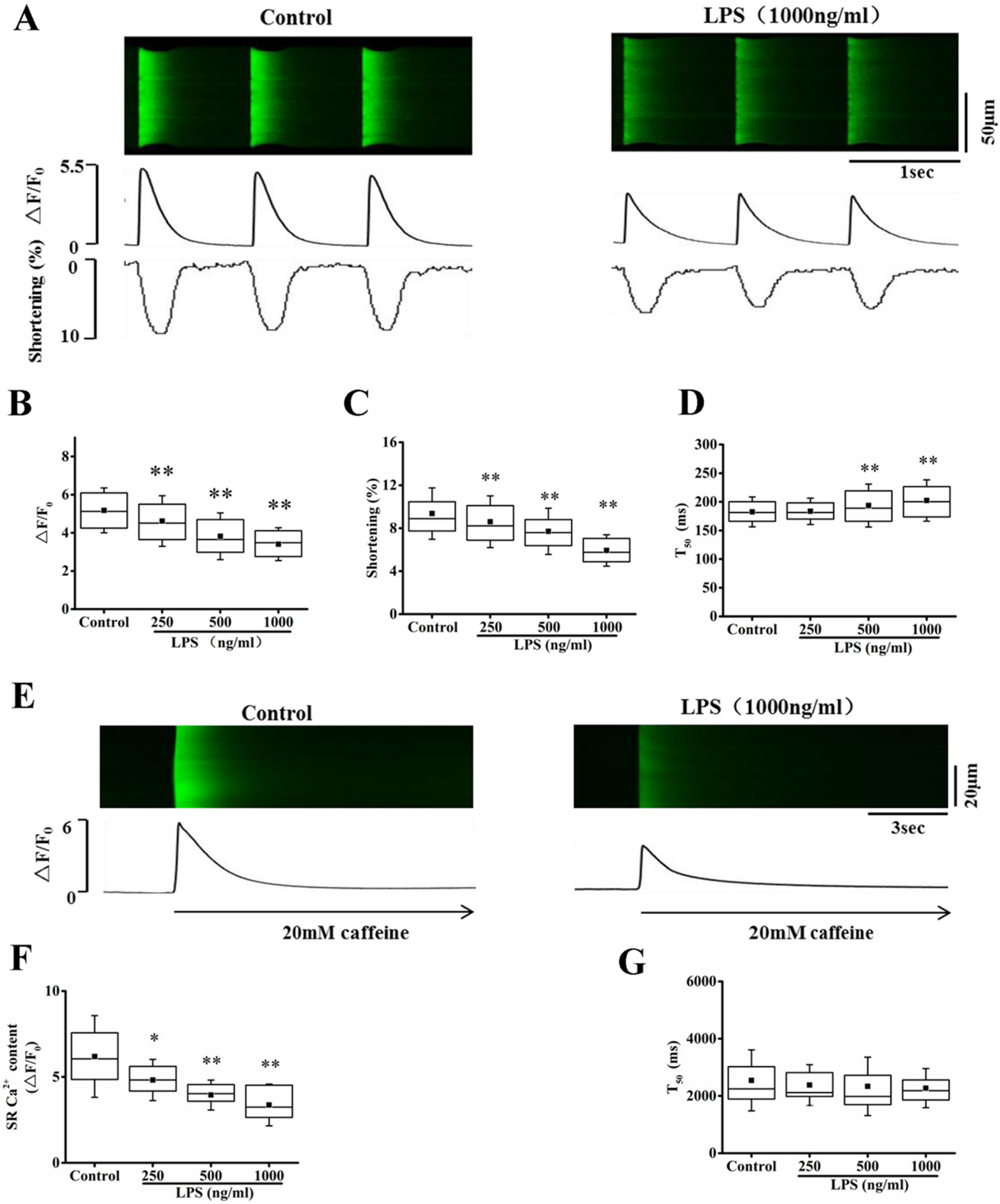

Figure 1. LPS decreased intracellular Ca^{2+} transient and myocyte contraction and decreased SR Ca^{2+} content in cardiomyocytes. *A*, representative confocal line-scan images of Ca^{2+} transient along with time courses of Ca^{2+} transient and cell shortening in control and LPS (1000 ng/ml)-treated cardiac myocyte paced at 1 Hz. *B* and *C*, average of the amplitude of Ca^{2+} transient ($\Delta F/F_0$; *B*) and percentage (%) of maximum cell shortening (*C*) in control and different doses (250–1000 ng/ml) of LPS-treated cells. *D*, average of the rise time (*bottom*) and half-time of decay (T_{50}; *top*) of Ca^{2+} transient. $n = 125–140$ cells in each group. *E*, representative images of caffeine-elicited Ca^{2+} transient in control and LPS (1000 ng/ml)-treated cardiac myocytes. *F*, statistics of the amplitude of caffeine-elicited Ca^{2+} transient (SR Ca^{2+} content) in control and different doses of LPS-treated cells. $n = 15–25$ cells in each group. *G*, half-time of decay (T_{50}) of caffeine-elicited Ca^{2+} transient ($n = 15–25$ cells in each group). *, $p < 0.05$; **, $p < 0.01$ *versus* control. *Error bars*, S.D.

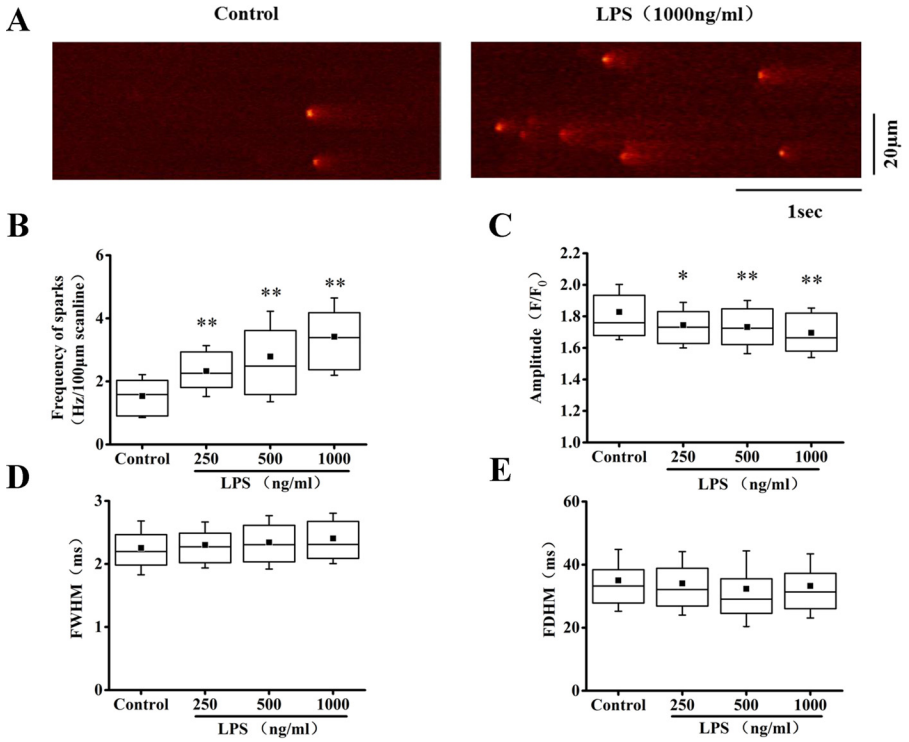

Figure 2. LPS increased Ca^{2+} sparks in cardiomyocytes. *A*, representative Ca^{2+} spark images in control and LPS (1000 ng/ml)-treated cells. *B*, average of the frequency of Ca^{2+} sparks in control and 250–1000 ng/ml LPS-treated cells. *C–E*, statistics of the amplitude (F/F_0; *C*), full width of half-maximum (*FWHM*; *D*), and full duration at half-maximum (*FDHM*; *E*) of Ca^{2+} sparks in control and LPS groups ($n = 53–75$ cells/group). *, $p < 0.05$; **, $p < 0.01$ *versus* control. *Error bars*, S.D.

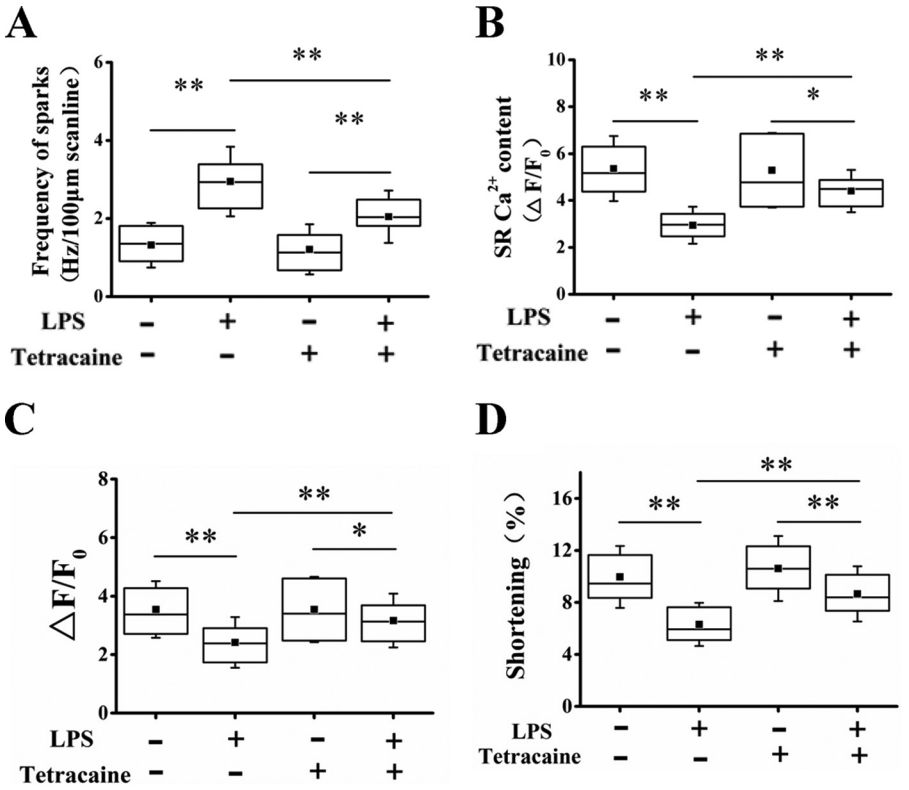

Figure 3. Effects of tetracaine on LPS modulation of Ca^{2+} handling and myocyte contraction in cardiomyocytes. *A–D*, statistics of the frequency of Ca^{2+} sparks ($n = 54–79$ in each group; *A*), the amplitude of caffeine-elicited Ca^{2+} transient (SR Ca^{2+} content, $n = 13–31$; *B*), the amplitude of action potential–elicited Ca^{2+} transient ($n = 39–58$; *C*), and maximum of cell shortening ($n = 39–58$; *D*) in control and LPS (1000 ng/ml)-treated cells with or without tetracaine (50 μM) pretreatment. *, $p < 0.05$; **, $p < 0.01$. *Error bars*, S.D. *Error bars*, S.D.

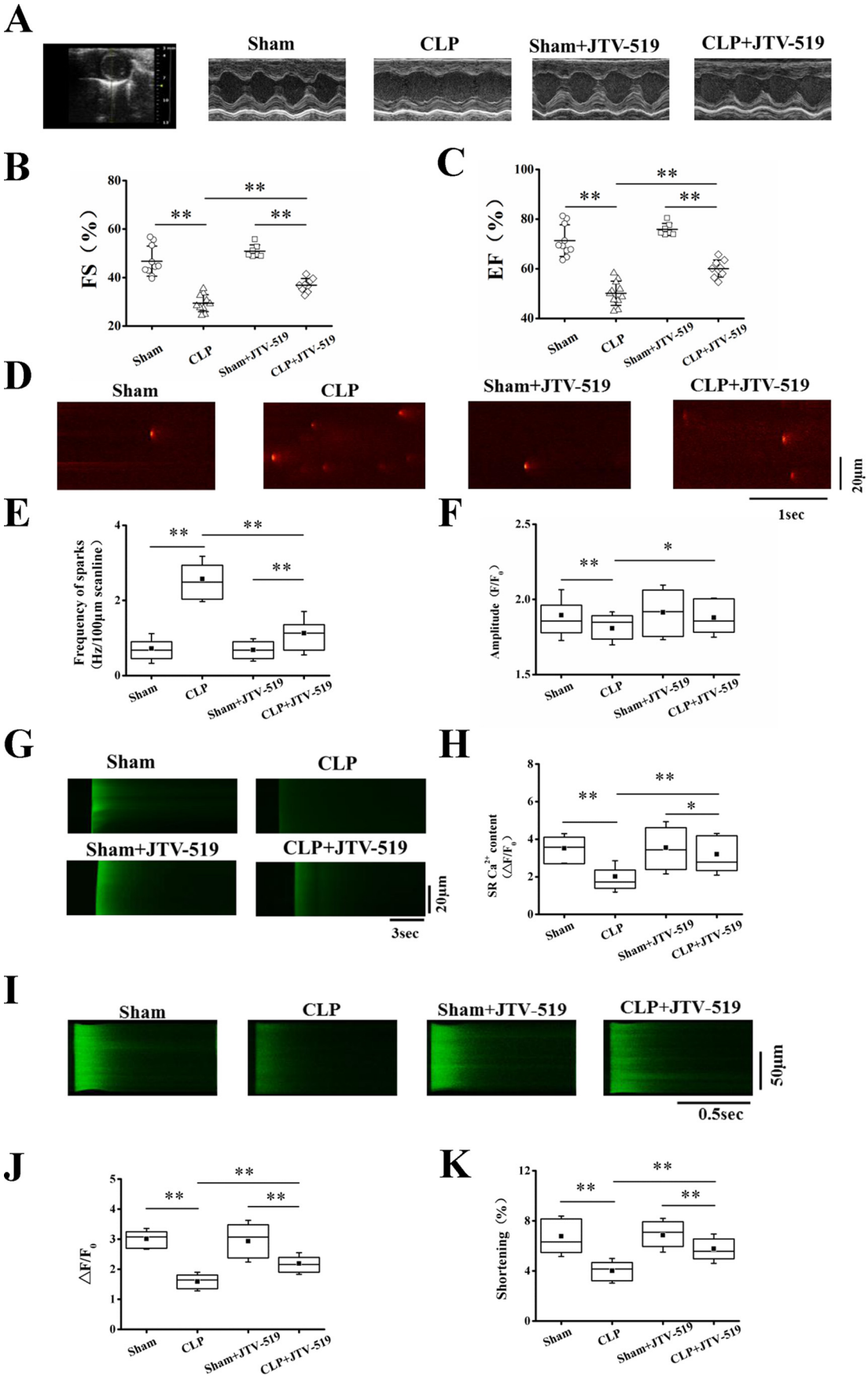
A
Sham
CLP
Sham+JTV-519
CLP+JTV-519
B
FS（%）
C
EF（%）
D
Sham
CLP
Sham+JTV-519
CLP+JTV-519
20μm
1sec
E
Frequency of sparks (Hz/100μm scanline)
F
Amplitude (F/F0)
G
Sham
CLP
Sham+JTV-519
CLP+JTV-519
20μm
3sec
H
SR Ca2+ content (ΔF/F0)
I
Sham
CLP
Sham+JTV-519
CLP+JTV-519
50μm
0.5sec
J
ΔF/F0
K
Shortening（%）

frequency of Ca^{2+} sparks was dramatically increased (Fig. 4, *D* and *E*), and the SR Ca^{2+} content (Fig. 4, *G* and *H*) and systolic intracellular Ca^{2+} transient and cell shortening (Fig. 4, *I–K*) were remarkably decreased. The results are consistent with the findings in LPS-treated cardiomyocytes.

JTV-519 is a newly developed 1,4-benzothiazepine drug with antiarrhythmic and cardioprotective properties relating to the role of preventing increased Ca^{2+} leak from the SR (26, 27). We thus explored the therapeutic effect of JTV-519 on the impaired contractility in septic cardiomyopathy by incubation of JTV-519 (1 μM) with cardiomyocytes from sham or CLP mice for 1 h (28, 29). Fig. 4 (*D* and *E*) demonstrates that JTV-519 significantly decreased the rate of Ca^{2+} sparks in cardiomyocytes isolated from septic mouse hearts. Concomitantly, JTV-519 restored the reduced SR Ca^{2+} content (Fig. 4, *G* and *H*) and increased the systolic Ca^{2+} transient and cell shortening (Fig. 4, *I–K*). JTV-519 applied *in vivo* (0.5 mg/kg/h, i.v., 2 h before the surgery) (30) improved cardiac function in CLP mice, where the EF and FS were significantly increased as compared with CLP mice without JTV-519 treatment (Fig. 4, *A–C*). Comparing the Ca^{2+} handling and myocyte contraction in cardiomyocytes isolated from CLP mice with or without JTV-519 treatment shows that the abnormal Ca^{2+} handling and the impaired myocyte contraction were largely corrected by JTV-519 treatment *in vivo* (Fig. S1). No matter whether it was applied *in vitro* or *in vivo*, JTV-519 had no significant effects on the production of pro-inflammatory cytokines, including IL-6, IL-1β, and TNF-α, which were increased in CLP mouse serum or in the cultural medium of septic cardiomyocytes (Fig. S2). The results confirm the central role of SR Ca^{2+} leak in impaired cardiac contractility in sepsis and highlight the therapeutic potential of JTV-519 in the treatment of septic cardiomyopathy.

Oxidative stress in RyR2 underlies the SR Ca^{2+} leak in LPS-treated cardiomyocytes

The occurrence of high-frequency Ca^{2+} spark under a low level of SR Ca^{2+} content indicates that the activity of RyR2 is increased by LPS. A series of studies demonstrates that oxidative modification of RyR2 leads to conformational change of RyR2 and thus alteration of RyR2 gating and open probability (28, 31, 32). Enhanced oxidative stress in RyR2 has been shown to be a major reason for SR Ca^{2+} leak in heart failure (28, 31–33). Therefore, we examined whether oxidative stress contributes to the increased RyR Ca^{2+} release in septic cardiomyopathy. As illustrated in Fig. 5 (*A* and *B*), the free thiol groups in RyR2 indicated by monobromobimane (mBB) fluorescence were significantly decreased in LPS-treated cells, indicating enhancement of oxidative stress in RyR2.

FK506-binding protein 1B (FKBP12.6) is an accessory protein of RyR2, and oxidative stress in RyR2 has been suggested to induce FKBP12.6 dissociation from RyR2, leading to hyperactive RyR2 in heart failure (34–36). We examined the content of FKBP12.6 associating with RyR2 in LPS-treated cardiomyocytes. The RyR2 complex was pulled down by co-immunoprecipitation with anti-RyR2 antibody. The protein levels of RyR2 and FKBP12.6 in the precipitations were quantified by Western blotting, and the ratio of FKBP12.6 to RyR2 was calculated to estimate the combination of FKBP12.6 with RyR2 (37–39). LPS treatment remarkably decreased the ratio of FKBP12.6 to RyR2 (Fig. 5, *C* and *D*). In contrast, LPS had no significant effect on the expression of FKBP12.6, where the total protein level of FKBP12.6 in the cell lysates indicated as the input remains unaltered by LPS treatment (Fig. 5*C*, *bottom*). The results indicate FKBP12.6 dissociation from RyR2 in response to LPS stimulation.

In cardiac myocytes, mitochondria occupy 30–40% of the cellular volume and constitute the major source of intracellular reactive oxygen species (ROS) production (40). It has been suggested that sepsis induces mitochondrial dysfunction, and mitochondria-derived ROS plays an important role in the development of septic cardiomyopathy (16, 41). To explore whether this accounts for the enhanced oxidative stress in RyR2 in LPS-treated cells, we examined the mitochondrial ROS (mitoROS) level indicated by the fluorescence intensity of 5-(and-6)-chloromethyl 2′,7′- dichlorodihydrofluorescein diacetate (MitoSOX) in control and LPS-stimulated cells. Fig. 5 (*E* and *F*) illustrates that LPS stimulation remarkably increased MitoSOX fluorescence. Using mito-TEMPO (25 μM, applied 60 min before LPS treatment) to scavenge mitoROS (Fig. 5, *E* and *F*) increased the free thiol groups in RyR2 (mBB fluorescence; Fig. 5, *A* and *B*) and the association of FKBP12.6 with RyR2 (Fig. 5, *C* and *D*) in LPS-stimulated cardiomyocytes. The LPS-induced high-frequency Ca^{2+} sparks were concomitantly suppressed (Fig. 5*G*). The results collectively indicate that mitoROS accumulation causes oxidative stress in RyR2 and FKBP12.6 dissociation from the channel, resulting in SR Ca^{2+} leak.

TLR4 mediates intracellular oxidative stress and SR leak

TLR4 is the receptor of LPS and plays a critical role in cardiac dysfunction in sepsis. TLR4-activated signaling pathways can induce mitochondrial dysfunction and excessive intracellular ROS accumulation (42). To explore the contribution of TLR4 activation in intracellular oxidative stress and consequent SR Ca^{2+} leak, we pretreated the cells with TLR4-specific inhibitor TAK-242 (1 μM) for 30 min before LPS stimulation. TAK-242

Figure 4. JTV-519 prevented Ca^{2+} spark–mediated SR Ca^{2+} leak and increased cardiac function in septic mice. A mouse model of polymicrobial sepsis was produced by CLP. *A*, representative images generated by echocardiography in sham and septic mice with or without JTV-519 treatment. JTV-519 (0.5 mg/kg/h) was applied intraperitoneally 2 h before the surgery. *B* and *C*, quantification of LV FS (*B*) and LV EF (*C*) in four groups (n = 7–13 in each group). *D*, representative images of Ca^{2+} spark in cardiomyocytes isolated from sham or septic mice with or without JTV-519 treatment. JTV-519 (1 μM) was incubated with sham or septic cardiomyocytes for 1 h before measurement of the Ca^{2+} spark, SR Ca^{2+} content, systolic Ca^{2+} transient, and cell shortening. *E* and *F*, statistics of the frequency and amplitude of Ca^{2+} sparks (n = 40–51 cells in each group). *G*, representative images of caffeine-elicited Ca^{2+} transient in cardiomyocytes isolated from sham or septic mice with or without JTV-519 treatment *in vitro*. *H*, statistics of the amplitude of caffeine-elicited Ca^{2+} transient (SR Ca^{2+} content; n = 24–28 cells in each group). *I*, representative confocal line-scan images of field stimulation (1 Hz)-induced Ca^{2+} transient in four groups. *J* and *K*, statistics of the amplitude of the systolic Ca^{2+} transient (*J*) and the maximum of cell shortening (*K*; n = 50–79 in each group). *, $p < 0.05$; **, $p < 0.01$. *Error bars*, S.D.

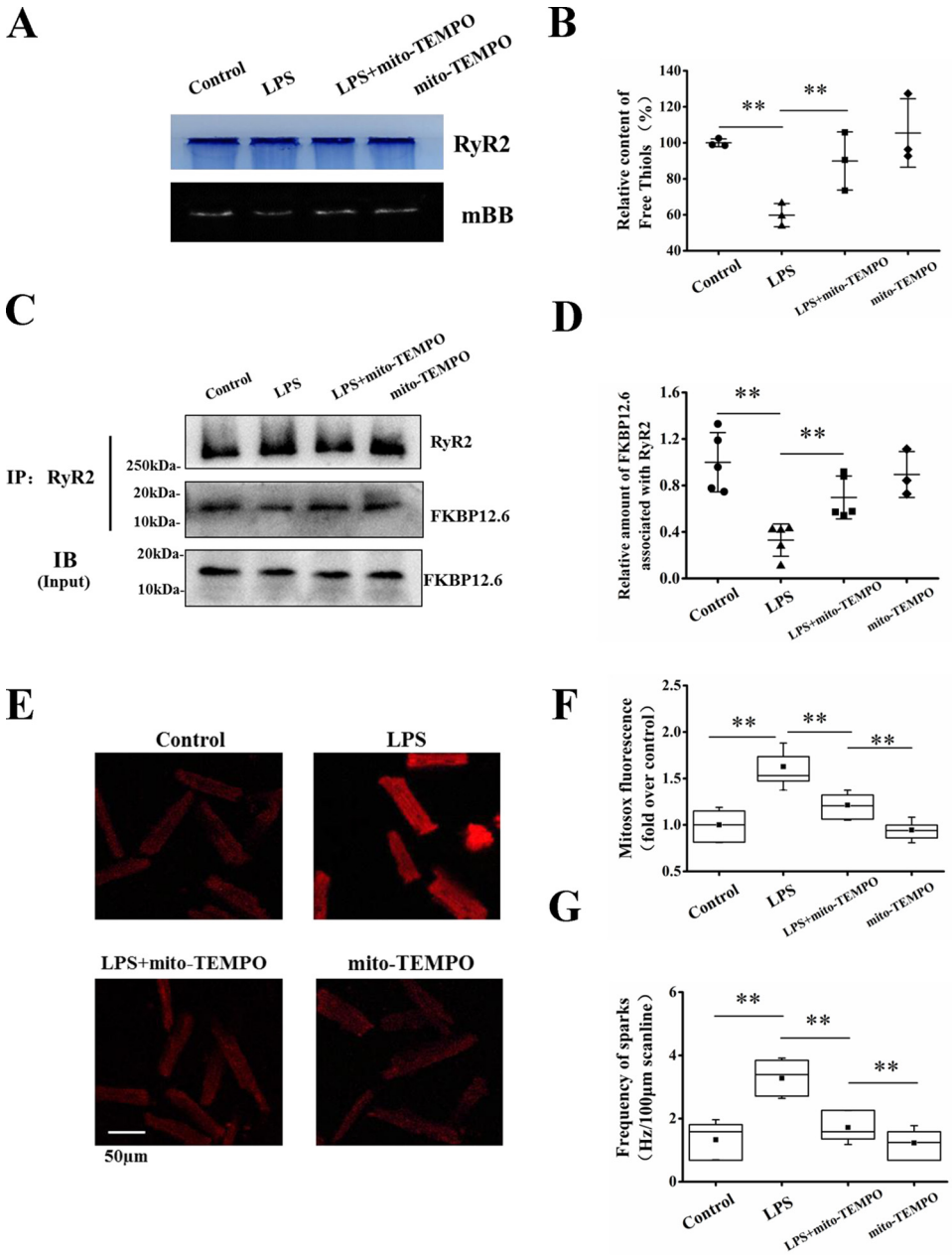

Figure 5. Effects of LPS on RyR2 oxidation, FKBP12.6 association with RyR2, and mitochondrial ROS generation. *A*, representative images of mBB fluorescence intensity and Coomassie-stained gels in parallel in control and LPS-treated cells with or without mito-TEMPO pretreatment. Mito-TEMPO (25 μM) was incubated with the cardiomyocytes for 60 min before LPS treatment to scavenge mitochondrial ROS. *B*, relative free thiol content (%) of RyR2 measured by normalizing mBB fluorescence to RyR2 level ($n = 3$ in each group). *C* and *D*, co-immunoprecipitation analysis of the relative amount of FKBP12.6 associated with RyR2. RyR2 complex was pulled down with anti-RyR2 antibody. Total cytosolic FKBP12.6 protein level indicated as input is shown in the *bottom panel*. The relative amount of FKBP12.6 associated with RyR2 was calculated as the ratio of the protein content of FKBP12.6 to RyR2 in the precipitation ($n = 3$–6 in each group). *E*, MitoSOX red fluorescence recorded from control, LPS, LPS + mito-TEMPO, and mito-TEMPO groups. *F*, averages of MitoSOX fluorescence in four groups ($n = 26$–50 cells in each group). *G*, averages of the frequency of Ca^{2+} sparks in four groups ($n = 30$–67 in each group). **, $p < 0.01$. *Error bars*, S.D. *IP*, immunoprecipitation; *IB*, immunoblotting.

largely inhibited LPS-induced increase of MitoSOX fluorescence (Fig. 6, *A* and *B*). The relative content of free thiol groups in RyR2 was significantly increased (Fig. 6, *C* and *D*). Furthermore, TAK-242 significantly reduced the high-frequency Ca^{2+} sparks stimulated by LPS (Fig. 6*E*). The results indicate that TLR4 mediates mitoROS production and oxidative stress in RyR2, resulting in enhancement of SR Ca^{2+} leak. With the correction of SR Ca^{2+} leak, TAK-242 increased SR Ca^{2+} content and intracellular Ca^{2+} transient and cell shortening in LPS-treated cells (Fig. 6, *F* and *G*).

Deletion of TLR4 improves cardiac function by preventing SR Ca^{2+} leak in septic mice

We further investigated the critical role of SR Ca^{2+} leak in TLR4-induced cardiac dysfunction in CLP septic mice with or without TLR4 gene knockout. Deletion of TLR4 ($TLR4^{-/-}$; Fig. 7, *A* and *B*) significantly increased cardiac function in the CLP mice, where EF and FS were increased by 32.5 and 42.1%, respectively, compared with WT CLP mice (Fig. 7*C*). The survival rate was significantly increased in $TLR4^{-/-}$ CLP mice (Fig. 7*D*).

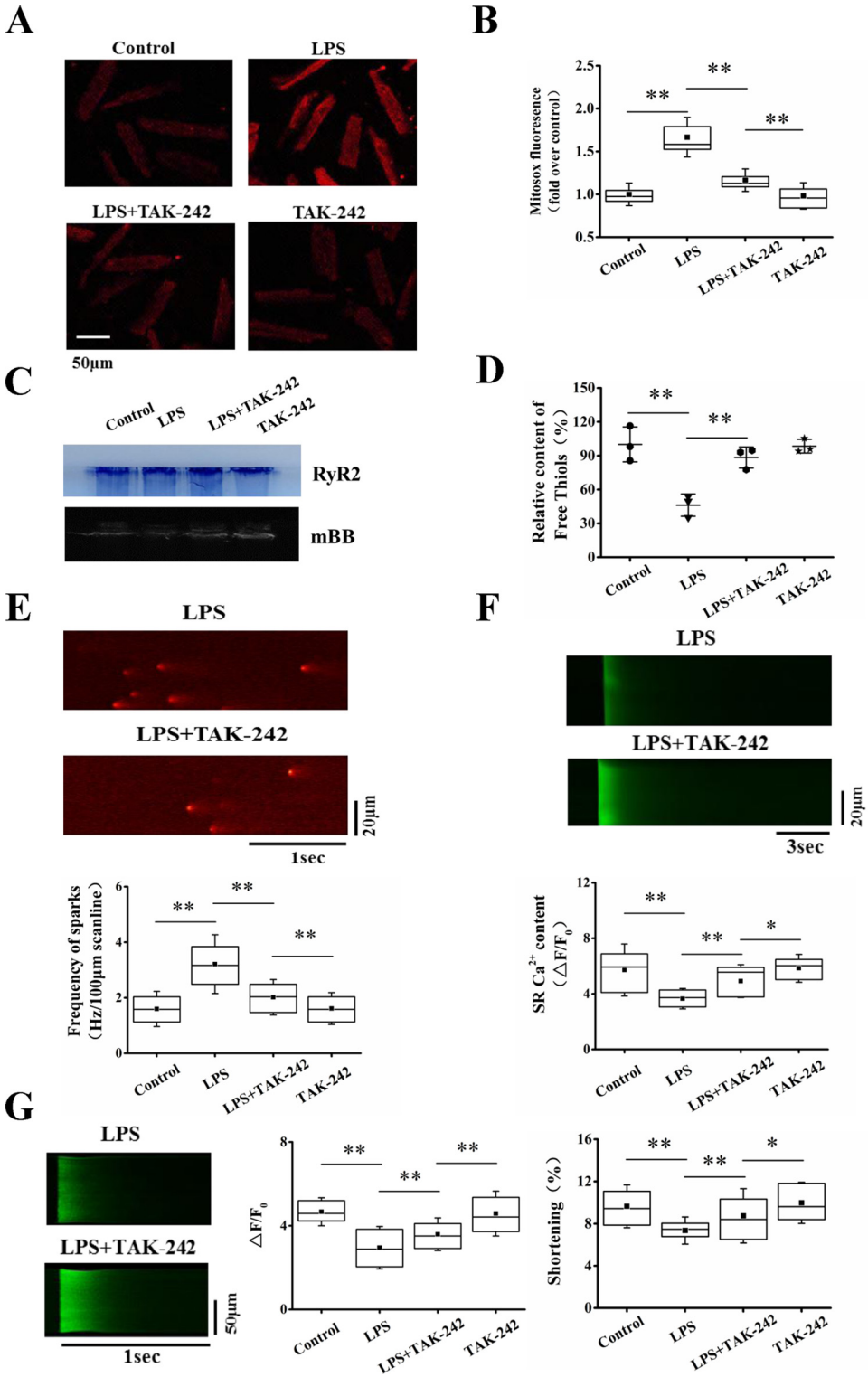

Figure 6. Blocking TLR4 inhibited intracellular oxidative stress and prevented SR Ca^{2+} leak in LPS-stimulated cardiomyocytes. *A*, representative images of MitoSOX red fluorescence recorded from control, LPS, LPS + TAK-242, and TAK-242 groups. *B*, averages of MitoSOX fluorescence in four groups (n = 38–49 cells in each group). *C*, representative images of mBB fluorescence intensity and Coomassie-stained gels in parallel in four groups. *D*, relative free thiol content (%) of RyR2 measured by normalizing mBB fluorescence to RyR2 level (n = 3 in each group). *E*, representative images and statistics of the frequency of Ca^{2+} sparks (n = 52–67 cells in each group). *F*, representative images and statistics of caffeine-elicited Ca^{2+} transient (n = 13–20 cells in each group). *G*, representative images and statistics of the amplitude of Ca^{2+} transient and the maximum of cell shortening (n = 37–50 in each group). *, $p < 0.05$; **, $p < 0.01$. *Error bars*, S.D.

The frequency of Ca^{2+} sparks in cardiomyocytes from *TLR4*$^{-/-}$ septic mice was much lower than that in cardiomyocytes from WT septic mice (Fig. 8*A*). Mirroring the decrease in Ca^{2+} spark–mediated SR leak, the SR Ca^{2+} content was remarkably increased in *TLR4*$^{-/-}$ septic mice compared with WT septic mice (Fig. 8*B*). Consistently, the systolic Ca^{2+} tran-

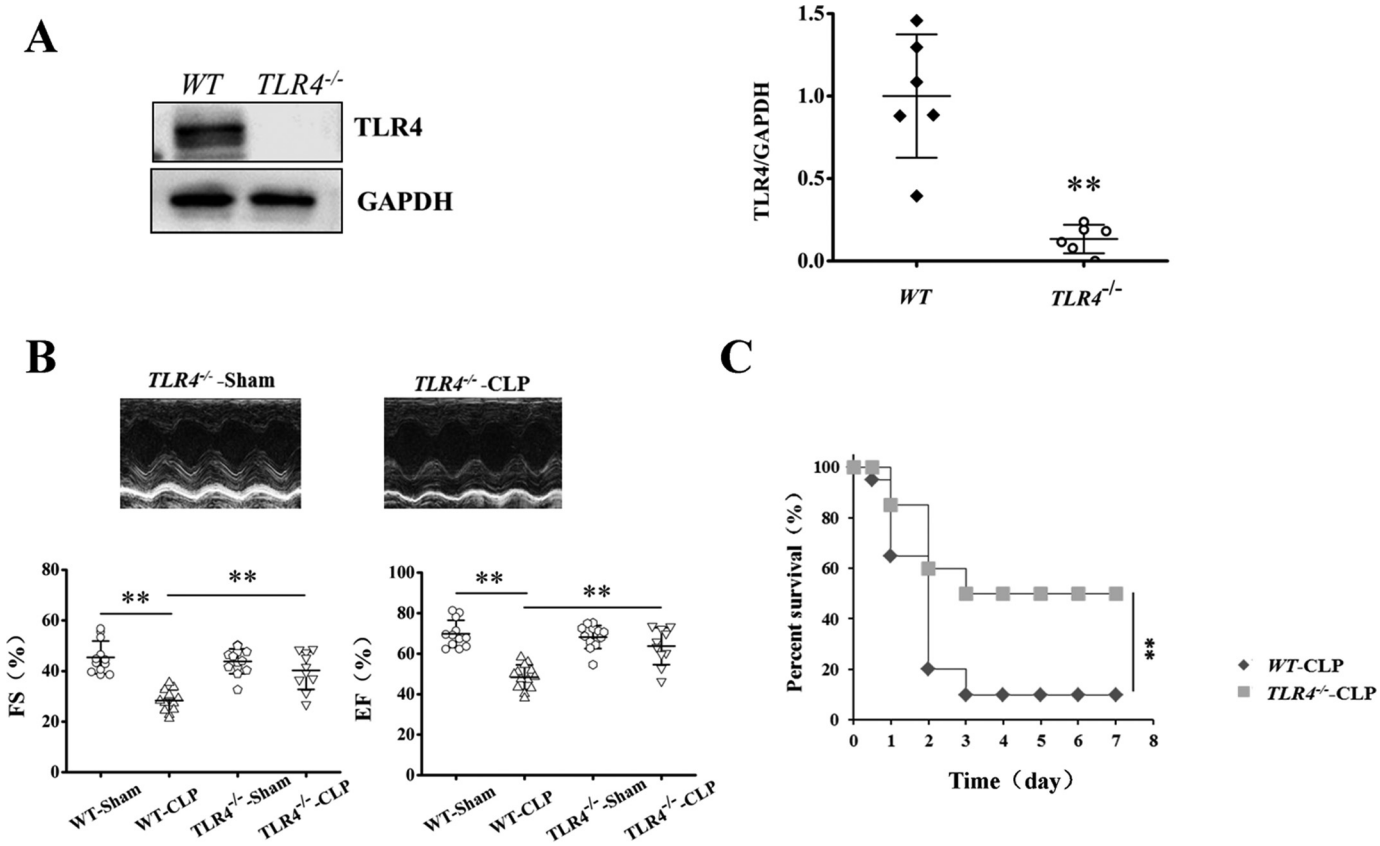

Figure 7. TLR4 deficiency attenuated cardiac dysfunction and increased survival rate in septic mice. *A*, representative images of Western blots of TLR4 and GAPDH proteins and statistics of TLR4 abundance in WT and *TLR4*$^{-/-}$ groups ($n = 6$ in each group). *B*, representative images generated by echocardiography and quantification of LV FS and LV EF ($n = 10–13$ in each group). *C*, TLR4 deficiency increases survival outcome in CLP-induced septic mice. *TLR4*$^{-/-}$ and age-matched WT mice (20 in each group) were subjected to CLP, and the survival was carefully monitored for half a day. **, $p < 0.01$. *Error bars*, S.D.

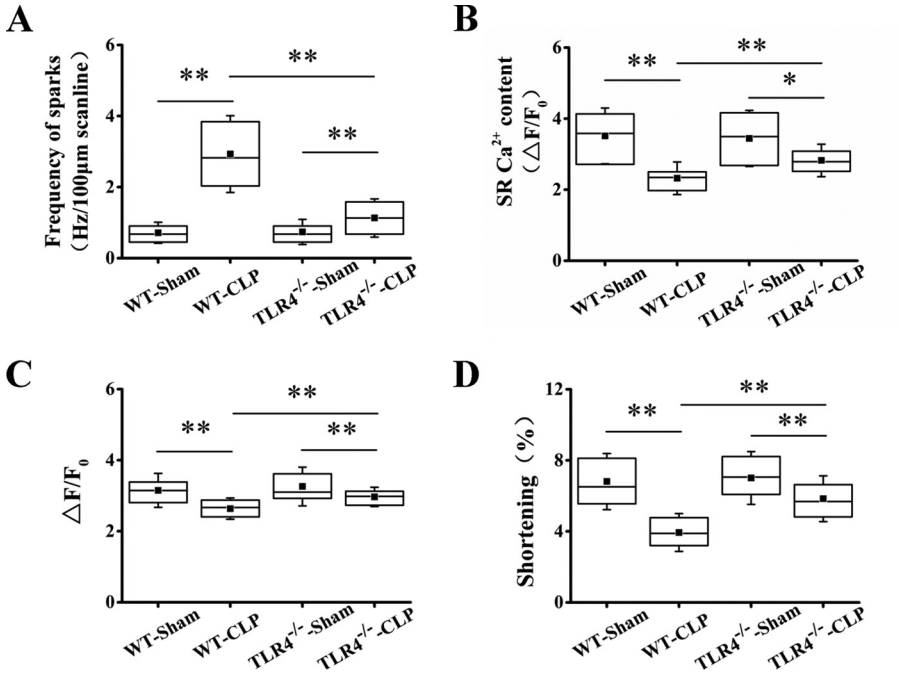

Figure 8. Deletion of TLR4 restores Ca^{2+} handling and myocyte contraction in septic mice. *A*, average of the frequency of Ca^{2+} sparks in WT-sham, WT-CLP, *TLR4*$^{-/-}$-sham, and *TLR4*$^{-/-}$-CLP groups ($n = 43–74$ in each group). *B*, statistics of the amplitude of SR Ca^{2+} content in four groups ($n = 16–28$ in each group). *C* and *D*, action potential–elicited Ca^{2+} transient and average of the peak Ca^{2+} transient (*C*) and maximum cell shortening (*D*; $n = 51–90$ in each group). *, $p < 0.05$; **, $p < 0.01$. *Error bars*, S.D.

sient and myocyte contractility were significantly increased (Fig. 8, *C* and *D*). The data indicate that TLR4 activation contributes to septic cardiac dysfunction through inducing SR Ca^{2+} leak.

Discussion

Enhancement of SR Ca^{2+} leak contributes to the contractile defect in septic cardiomyopathy

One major finding in this study is strong evidence indicating that enhancement of Ca^{2+} spark–mediated SR Ca^{2+} leak plays a critical role in the contractile dysfunction in septic cardiomyopathy. There are three types of supporting evidence. First, LPS, the major cause of sepsis, increased Ca^{2+} spark–mediated SR Ca^{2+} leak but decreased SR Ca^{2+} content, systolic Ca^{2+} transient, and cell shortening in cardiomyocytes. Preventing the SR leak with RyR blocker, tetracaine restored SR Ca^{2+} content and significantly increased systolic Ca^{2+} transient and cell shortening. The results indicate the causal relationship between the increased SR Ca^{2+} leak and the decreased SR Ca^{2+} content and the resulting contractile dysfunction in LPS-treated cardiomyocytes. Second, preventing the hyperactive Ca^{2+} spark–mediated SR leak with JTV-519 restored the SR Ca^{2+} content and increased systolic Ca^{2+} transient and myocyte contraction in mouse septic cardiomyopathy. Third, blocking or deletion of TLR4, the critical molecule mediating SR Ca^{2+} leak, corrected the abnormal Ca^{2+} handling and myocyte contraction in septic cardiomyopathy. Therefore, we conclude that enhancement of SR Ca^{2+} leak plays a critical role in the contractile defect in septic cardiomyopathy through partially depleting SR Ca^{2+} content.

TLR4-mediated oxidative stress in RyR2 underlies the enhancement of SR Ca^{2+} leak

The enhancement of SR Ca^{2+} leak can be attributed to increased SR Ca^{2+} content and hyperactive RyR activity. Given that SR Ca^{2+} content was decreased in septic cardiomyopathy and restored when the abnormal SR Ca^{2+} leak was corrected, it is the result rather than the cause of the enhancement of SR Ca^{2+} leak. Therefore, the SR Ca^{2+} leak can only be induced by increasing RyR activity. It is known that RyR2 is rich in cysteines and sensitive to oxidative modification. Oxidative stress in RyR2 changes the channel gating, which has been linked to enhancement of RyR Ca^{2+} leak in failing heart (17, 18, 28). In septic cardiomyocytes, we similarly found increased oxidative stress in RyR2. Reducing the oxidative stress largely decreased the frequency of Ca^{2+} sparks. Therefore, oxidative modification of RyR2 is a major reason for Ca^{2+} spark–mediated SR Ca^{2+} leak in septic cardiomyopathy.

There are multiple sources of ROS in cardiac myocytes, where mitochondria occupy 30–40% of the cellular volume and constitute the major source of intracellular ROS production (40). Mitochondrial dysfunction has been shown to play a critical role in the development of septic cardiomyopathy (16, 41, 42). In this study, we found that excessive mitochondria-derived ROS was accumulated in septic cardiomyocytes. Scavenging the accumulated mitochondrial ROS with mito-TEMPO relieved oxidative stress in RyR2, indicating that mitochondrial dysfunction contributes largely to the oxidative stress in RyR2 in septic cardiomyopathy.

The TLR4-mediated signaling pathways play a critical role in sepsis-induced cardiac dysfunction through inducing inflammation and ROS production (43). Recent studies have linked TLR4 signaling to mitochondrial dysfunction, where the activation of TLR4 induces mitochondrial ROS generation by interfering with mitochondrial respiratory chain (44). In septic cardiomyocytes, we found that inhibition or deletion of TLR4 decreased mitochondrial ROS production, prevented Ca^{2+} spark–mediated SR Ca^{2+} leak, and improved cardiac function in septic cardiomyopathy. Taken together, we conclude that TLR4 plays a critical role in inducing SR Ca^{2+} leak in septic cardiomyocytes. Activation of TLR4 stimulates mitochondrial ROS generation and enhances oxidative stress in RyR2, leading to hyperactive RyR2 and subsequent SR Ca^{2+} leak. Despite the direct effect of ROS on increasing RyR2 activity, it may also act through activating Ca^{2+}/calmodulin-dependent kinase II, which increases RyR activity by phosphorylation of RyR2 (45).

Possible role of FKBP12.6 dissociation in the oxidative stress-induced SR Ca^{2+} leak

FKBP12.6 is an accessory protein of RyR2, and the dissociation of FKBP12.6 from RyR2 has been shown to cause SR Ca^{2+} leak in heart failure in previous studies (34, 46). In septic cardiomyocytes, we found that oxidative stress in RyR2 induces FKBP12.6 dissociation from RyR2. Relieving oxidative stress in RyR2 restored the interaction of FKBP12.6 with RyR2, suggesting that FKBP12.6 dissociation may be an important link for oxidative stress-induced SR Ca^{2+} leak in septic cardiomyopathy.

Of note, the reports on the role of FKBP12.6 in the gating of RyR2 and the regulation of SR Ca^{2+} release are extremely controversial because RyRs are intracellular channels inaccessible to direct electrophysiological measurements. Lipid bilayers have been widely used to study the role of FKBP12.6 in RyR gating at the single-channel level. However, the experimental setting has the shortcoming of not being able to reconstruct the native environment, such as the interacting proteins (calsequestrin, junctin, triadin, etc.) and the exact intracellular ionic composition. Thus, the results vary greatly among laboratories. Single RyRs from FKBP12.6-knockout mice or treated with rapamycin/FK506 to dissociate FKBP12.6 were found to have increased open probability and partial opening/subconductance in some studies but not in others (47–50). In intact cardiomyocytes, the role of FKBP12.6 in the regulation of SR Ca^{2+} release is studied by observing Ca^{2+} sparks; however, it is still highly controversial. Xin *et al.* (51) demonstrated that FKBP12.6 knockout increases the amplitude and duration but not the frequency of Ca^{2+} sparks. By contrast, some reports have shown that FK506 treatment or FKBP12.6 dissociation increases the spontaneous Ca^{2+} spark frequency (52). FKBP12.6 knockout mice develop lethal arrhythmia during exercise (53). A recent study by Zhao *et al.* (54) demonstrated that FKBP12.6 dissociation increases the frequency but not the amplitude and kinetics of Ca^{2+} sparks by using a combination of FKBP12.6-knockout mice and FK506/rapamycin pharmacology. As reported by a previous study, only <20% of

FKBP12.6 binding sites on RyRs are occupied by FKBP12.6 (55), which calls into question the critical role of FKBP12.6 in the regulation of normal RyR2. Recent structural analysis has indicated that FKBP is inserted into the gap between the JSol (handle) domain and SPRY triangle of RyR (56–59). Based on these findings, Zhao *et al.* (54) proposed a model in which a single-subunit occupation of FKBP12.6 stabilizes two adjacent subunits of an RyR (which has four FKBP12.6-binding sites on its four subunits), and a ~20% occupation of FKBP12.6-binding sites stabilizes ~59% of RyRs to explain the robust effect of FKBP12.6 knockout on RyR2 activity. Nevertheless, we may not exclude the possibility that oxidative stress in the RyR2 channel itself mediates the SR Ca^{2+} leak in septic cardiomyopathy, and the role of FKBP12.6 is minor in view of the extremely controversial reports on the role of FKBP12.6 in regulating RyR gating and SR Ca^{2+} release.

In summary, this study provides direct evidence indicating the critical role of Ca^{2+} spark–mediated SR Ca^{2+} leak in the development of septic cardiomyopathy. Mechanistically, the activation of the signal axis, TLR4–mitoROS accumulation–enhancement of RyR2 oxidative stress, induces hyperactive RyR2 and the increased SR Ca^{2+} leak. The dissociation of FKBP12.6 from RyR2 may participate in but not be essential to oxidative stress-induced RyR2 hyperactivity. Furthermore, this study demonstrates for the first time the therapeutic potential of JTV-519 in the treatment of septic cardiomyopathy by preventing SR Ca^{2+} leak.

Materials and methods

Animals and CLP model

Adult Sprague-Dawley rats of either sex, weighing 200–220 g, and wild-type male C57BL/6 mice weighing 18–22 g were purchased from the Animal Center of Southern Medical University, and *TLR4*$^{-/-}$ mice were purchased from the Model Animal Research Center of Nanjing University. All animal experiments were handled in accordance with a protocol approved by the institutional care and use committee of Shenzhen University, which conforms to the ethical standards formulated in the Guide for the Care and Use of Laboratory Animals published by the National Institutes of Health (NIH Publication 85-23, revised 1996). CLP was performed to induce sepsis in mice as described previously (60). In brief, the animal was endotracheally intubated under deep anesthesia with a mixture of pentobarbital sodium (50 mg/kg, i.p.). The abdominal cavity was opened, and the distal 1 cm of the cecum was ligated with a suture and punctured twice with a needle of 16 gauge. After surgery, all mice received a 1-ml subcutaneous injection of physiological saline. As controls, sham-operated mice received the same procedures except for ligation and puncture.

Echocardiography

2D guided M-mode echocardiography was performed in anesthetized mice (with 1.5% isoflurane) using a Vevo 2100 system (VisualSonics, Toronto, Canada). The heart was imaged in the 2D mode in the parasternal short-axis view. From this view, the LV internal dimensions at both diastole and systole (LVIDd and LVIDs, respectively) were measured. All measurements were done from leading edge to leading edge according to the American Society of Echocardiography guidelines. The percentage of LV FS (%) was calculated as ((LVIDd − LVIDs)/LVIDd) × 100, and LV EF (%) was calculated as (($LVIDd^2$ − $LVIDs^2$)/$LVIDd^2$) × 100.

Isolation of adult rat ventricular myocytes

Adult rat ventricular myocytes were isolated from adult SD rats as described previously (19, 61). Briefly, after deep anesthesia with trichloroacetaldehyde monohydrate (0.5 g/kg, i.p.), the heart was quickly removed from the rat chest; cleaned and flushed with nominally Ca^{2+}-free Tyrode solution consisting of 137 mM NaCl, 5.4 mM KCl, 1.2 mM $MgCl_2$, 1.2 mM NaH_2PO_4, 10 mM glucose, and 20 mM HEPES (pH 7.3, adjusted with NaOH); and perfused using a Langendorff apparatus at 37 °C. After 5 min, the solution was switched to the enzyme solution with 0.5 mg/ml collagenase (Worthington; Type II) and 0.06 mg/ml protease (Sigma; Type XIV) for 15 min. All solutions were equilibrated with 100% O_2. Then the heart was minced into small chunks, and single cells were shaken loose from the heart tissue and stored in HEPES-buffered external solution containing 137 mM NaCl, 5.4 mM KCl, 1 mM $CaCl_2$, 1.2 mM $MgCl_2$, 1.2 mM NaH_2PO_4, 20 mM glucose, and 20 mM HEPES (pH 7.4).

Isolation of adult mouse ventricular myocytes

Adult mouse ventricular myocytes were isolated from anesthetized C57BL/6 mice as described previously (62). Briefly, the heart was quickly removed and cleaned and flushed with a Ca^{2+}-free buffer containing 120 mM NaCl, 5.4 mM KCl, 1.2 mM $MgSO_4$, 1.2 mM NaH_2PO_4, 5.6 mM glucose, 20 mM $NaHCO_3$, 10 mM 2,3-butanedione monoxime (BDM; Sigma), 5 mM taurine, 10 mM HEPES (pH 7.4) and perfused using a Langendorff apparatus. All solutions were bubbled with 100% O_2. The enzymatic digestion was initiated by adding collagenase type B (0.75 mg/ml; Worthington) and protease type XIV (0.02 mg/ml; Sigma) to the perfusion solution. When the heart became swollen and hard after 3 min of digestion, 50 μM Ca^{2+} was added to the enzyme solution and perfused for about 30 min. Following the perfusion procedure, the heart was minced into small chunks, and single cells were shaken loose from the heart tissue and stored in HEPES-buffered solution containing 1 mM $CaCl_2$, 137 mM NaCl, 5.4 mM KCl, 15 mM dextrose, 1.3 mM $MgSO_4$, 1.2 mM NaH2PO$_4$, and 20 mM HEPES, adjusted to pH 7.4 with NaOH. Cells were used for the following experiments within 4 h after isolation.

Ca^{2+} spark and Ca^{2+} transient detection and contraction measurement

Isolated ventricular myocytes loaded with Ca^{2+} indicator Fluo-4 AM (5 μmol/liter at room temperature for 8 min) (Invitrogen) were placed in a recording chamber. Ca^{2+} sparks and transients were recorded as reported previously (19). For Ca^{2+} spark recording, confocal line-scan imaging was carried out in resting cells at 488-nm excitation and 505-nm collection with a Zeiss 710 inverted confocal microscope (Carl Zeiss, Oberkochen, Germany) with a ×40 oil immersion lens (numerical aperture 1.3). Line-scan images were acquired at a sampling rate of 3.84 ms/line, along the longitudinal axis of the cell. For

the detection of systolic Ca^{2+} transient, after the cells were stimulated with field stimulation (1 Hz) to reach a steady state, confocal line-scan imaging was performed with the same confocal parameters used for Ca^{2+} spark recording under field stimulation (1 Hz). Myocyte contraction was measured by detecting the length of two edges of the cell along with the time of stimulation. Myocytes were superfused with HEPES-buffered external solution during the experiment.

Measurement of SR Ca^{2+} load

Short puffs of caffeine (20 mmol/liter) were applied to completely empty the SR, following a train of 1-Hz field stimulation to achieve steady-state SR Ca^{2+} loading in ventricular myocytes. SR Ca^{2+} content was assessed by detecting the amplitude of a caffeine-elicited Ca^{2+} transient. Cells were superfused with HEPES-buffered external solution.

Measurement of ROS in mitochondria

Isolated cardiomyocytes were loaded with 5 μM MitoSOX (Invitrogen) for 15 min at room temperature (63, 64). Frame fluorescence images (excitation at 488 nm and emission at 505–530 nm, laser intensity 4%, 6.6 s/frame) were acquired with a Zeiss 710 inverted confocal microscope with ×40 lens. Because MitoSOX is light-sensitive and oxidized progressively, we used the same scanning parameters for all of the related experiments.

Oxidative stress level in RyR2

The content of the free thiols (*i.e.* the number of reduced cysteines) in RyR2 in cardiomyocytes was determined with the mBB (Calbiochem) fluorescence technique (17, 28). Heavy SR vesicles were prepared from different groups of cells under non-reducing conditions. Samples were incubated with 400 μmol/liter mBB for 1 h in the dark at room temperature. Then proteins were acetone-precipitated and subjected to SDS-PAGE (in a 6% polyacrylamide gel). The mBB fluorescence was measured using BIO-PEOFLL (Vilber Lourmat Biotechnology (Marne-la-Vallé, France); excitation 365 nm and emission 400–600 nm). Images were acquired and analyzed using Biocapt software. After that, the same gel was stained with Coomassie Blue. The mBB fluorescence in the RyR2 (~560 kDa) was normalized by protein abundance of RyR2 determined by Coomassie Blue staining of the same gel, which was defined as the relative content of free thiols in the RyR2.

Co-immunoprecipitation and Western blotting to detect the relative amount of FKBP12.6 associated with RyR2

We examined FKBP12.6 association with RyR2 as described previously (37, 38). Briefly, cardiomyocytes were lysed in modified radioimmune precipitation lysis buffer, shaking on ice for 20 min. The lysates were centrifuged at 12,000 × *g* for 15 min at 4 °C. The supernatants were collected, and the protein concentrations were determined with a bicinchoninic acid (BCA) protein assay kit (Thermo Fisher Scientific). The 100 μg of supernatant protein was incubated with 2 μg of anti-RyR2 antibody (Abcam) in 0.1 ml of modified radioimmune precipitation buffer and shaken slowly overnight at 4 °C. The samples were incubated with 40 μl of protein A/G-agarose beads at 4 °C for 3 h. The resins were washed three times with radioimmune precipitation buffer, and the eluted immunoprecipitated proteins were boiled for 5 min at 95 °C and loaded into wells in the 10% SDS-PAGE before being transferred to PVDF membranes and then probed with primary antibody: anti-RyR2 (1:1000; Abcam), FKBP12.6 (1:2000; Elabscience). Bound antibodies were visualized using the enhanced chemiluminescence (ECL) detection kit (Beyotime). The FKBP12.6 associated with RyR2 was calculated as the ratio of FKBP12.6 to RyR2 protein content in RyR2 immunoprecipitates. Total FKBP12.6 protein level in cell lysates was detected as input to indicate the expression level of FKBP12.6.

Data analysis

All values were expressed as means ± S.D. Statistical analyses were performed by unpaired two-tailed *t* test or one-way analysis of variance when appropriate, using SPSS Statistics version 20.0 software (IBM Corp., Armonk, NY). Values of $p < 0.05$ were considered statistically significant.

Author contributions—J. Liu conceived and coordinated the study and wrote the paper. J. Y., R. Z., and X. J. performed and analyzed the experiments shown in Figs. 1–8. J. Lv, Y. L., H. Y., W. L., C. Z., N. Z., M. D., Y. W., P. C., and K. S. participated in the experiments shown in Figs. 4, 7, and 8. Y. J. and G. W. provided technical assistance and contributed to the preparation of the figures. Y. J. also participated in the coordination of this paper. All authors reviewed the results and approved the final version of the manuscript.

References

1. Du, B., An, Y., Kang, Y., Yu, X., Zhao, M., Ma, X., Ai, Y., Xu, Y., Wang, Y., Qian, C., Wu, D., Sun, R., Li, S., Hu, Z., Cao, X., *et al.* (2013) Characteristics of critically ill patients in ICUs in mainland China. *Crit. Care Med.* **41,** 84–92 CrossRef Medline
2. Fleischmann, C., Scherag, A., Adhikari, N. K., Hartog, C. S., Tsaganos, T., Schlattmann, P., Angus, D. C., Reinhart, K., and International Forum of Acute Care Trialists (2016) Assessment of global incidence and mortality of hospital-treated sepsis: current estimates and limitations. *Am. J. Respir. Crit. Care Med.* **193,** 259–272 CrossRef Medline
3. Raj, S., Killinger, J. S., Gonzalez, J. A., and Lopez, L. (2014) Myocardial dysfunction in pediatric septic shock. *J. Pediatr.* **164,** 72–77.e2 CrossRef Medline
4. Bers, D. M. (2002) Cardiac excitation-contraction coupling. *Nature* **415,** 198–205 CrossRef Medline
5. Bers, D. M., and Guo, T. (2005) Calcium signaling in cardiac ventricular myocytes. *Ann. N.Y. Acad. Sci.* **1047,** 86–98 CrossRef Medline
6. Gao, H., Wang, F., Wang, W., Makarewich, C. A., Zhang, H., Kubo, H., Berretta, R. M., Barr, L. A., Molkentin, J. D., and Houser, S. R. (2012) Ca^{2+} influx through L-type Ca^{2+} channels and transient receptor potential channels activates pathological hypertrophy signaling. *J. Mol. Cell Cardiol.* **53,** 657–667 CrossRef Medline
7. Wang, W., Zhang, H., Gao, H., Kubo, H., Berretta, R. M., Chen, X., and Houser, S. R. (2010) β_1-Adrenergic receptor activation induces mouse cardiac myocyte death through both L-type calcium channel-dependent and -independent pathways. *Am. J. Physiol. Heart Circ. Physiol.* **299,** H322–H331 CrossRef Medline
8. Bers, D. M. (2000) Calcium fluxes involved in control of cardiac myocyte contraction. *Circ. Res.* **87,** 275–281 CrossRef Medline
9. Cheng, H., and Wang, S. Q. (2002) Calcium signaling between sarcolemmal calcium channels and ryanodine receptors in heart cells. *Front. Biosci.* **7,** d1867–d1878 CrossRef Medline
10. Lukyanenko, V., Viatchenko-Karpinski, S., Smirnov, A., Wiesner, T. F., and Györke, S. (2001) Dynamic regulation of sarcoplasmic reticulum Ca^{2+}

content and release by luminal Ca^{2+}-sensitive leak in rat ventricular myocytes. *Biophys. J.* **81,** 785–798 CrossRef Medline

11. Duncan, D. J., Yang, Z., Hopkins, P. M., Steele, D. S., and Harrison, S. M. (2010) TNF-α and IL-1β increase Ca^{2+} leak from the sarcoplasmic reticulum and susceptibility to arrhythmia in rat ventricular myocytes. *Cell Calcium* **47,** 378–386 CrossRef Medline
12. Yang, Z., Harrison, S. M., and Steele, D. S. (2005) ATP-dependent effects of halothane on SR Ca^{2+} regulation in permeabilized atrial myocytes. *Cardiovasc. Res.* **65,** 167–176 CrossRef Medline
13. Bode, E. F., Briston, S. J., Overend, C. L., O'Neill, S. C., Trafford, A. W., and Eisner, D. A. (2011) Changes of SERCA activity have only modest effects on sarcoplasmic reticulum Ca^{2+} content in rat ventricular myocytes. *J. Physiol.* **589,** 4723–4729 CrossRef Medline
14. Kuster, G. M., Lancel, S., Zhang, J., Communal, C., Trucillo, M. P., Lim, C. C., Pfister, O., Weinberg, E. O., Cohen, R. A., Liao, R., Siwik, D. A., and Colucci, W. S. (2010) Redox-mediated reciprocal regulation of SERCA and Na^+-Ca^{2+} exchanger contributes to sarcoplasmic reticulum Ca^{2+} depletion in cardiac myocytes. *Free Radic. Biol. Med.* **48,** 1182–1187 CrossRef Medline
15. Zhu, X., Bernecker, O. Y., Manohar, N. S., Hajjar, R. J., Hellman, J., Ichinose, F., Valdivia, H. H., and Schmidt, U. (2005) Increased leakage of sarcoplasmic reticulum Ca^{2+} contributes to abnormal myocyte Ca^{2+} handling and shortening in sepsis. *Crit. Care Med.* **33,** 598–604 CrossRef Medline
16. Cimolai, M. C., Alvarez, S., Bode, C., and Bugger, H. (2015) Mitochondrial mechanisms in septic cardiomyopathy. *Int. J. Mol. Sci.* **16,** 17763–17778 CrossRef Medline
17. Terentyev, D., Györke, I., Belevych, A. E., Terentyeva, R., Sridhar, A., Nishijima, Y., de Blanco, E. C., Khanna, S., Sen, C. K., Cardounel, A. J., Carnes, C. A., and Györke, S. (2008) Redox modification of ryanodine receptors contributes to sarcoplasmic reticulum Ca^{2+} leak in chronic heart failure. *Circ. Res.* **103,** 1466–1472 CrossRef Medline
18. Kubalova, Z., Terentyev, D., Viatchenko-Karpinski, S., Nishijima, Y., Györke, I., Terentyeva, R., Da Cuñha, D., Sridhar, A., Feldman, D. S., Hamlin, R. L., Carnes, C. A., and Györke, S. (2005) Abnormal intrastore calcium signaling in chronic heart failure. *Proc. Natl. Acad Sci. U.S.A.* **102,** 14104–14109 CrossRef Medline
19. Deng, J., Wang, G., Huang, Q., Yan, Y., Li, K., Tan, W., Jin, C., Wang, Y., and Liu, J. (2008) Oxidative stress-induced leaky sarcoplasmic reticulum underlying acute heart failure in severe burn trauma. *Free Radic. Biol. Med.* **44,** 375–385 CrossRef Medline
20. Zhang, C., Mo, M., Ding, W., Liu, W., Yan, D., Deng, J., Luo, X., and Liu, J. (2014) High-mobility group box 1 (HMGB1) impaired cardiac excitation-contraction coupling by enhancing the sarcoplasmic reticulum (SR) Ca^{2+} leak through TLR4-ROS signaling in cardiomyocytes. *J. Mol. Cell Ccardiol.* **74,** 260–273 CrossRef Medline
21. Li, H., Hu, D., Fan, H., Zhang, Y., LeSage, G. D., Caudle, Y., Stuart, C., Liu, Z., and Yin, D. (2014) β-Arrestin 2 negatively regulates Toll-like receptor 4 (TLR4)-triggered inflammatory signaling via targeting p38 MAPK and interleukin 10. *J. Biol. Chem.* **289,** 23075–23085 CrossRef Medline
22. Venetucci, L. A., Trafford, A. W., Díaz, M. E., O'Neill, S. C., and Eisner, D. A. (2006) Reducing ryanodine receptor open probability as a means to abolish spontaneous Ca^{2+} release and increase Ca^{2+} transient amplitude in adult ventricular myocytes. *Circ. Res.* **98,** 1299–1305 CrossRef Medline
23. Gao, M., Ha, T., Zhang, X., Liu, L., Wang, X., Kelley, J., Singh, K., Kao, R., Gao, X., Williams, D., and Li, C. (2012) Toll-like receptor 3 plays a central role in cardiac dysfunction during polymicrobial sepsis. *Crit. Care Med.* **40,** 2390–2399 CrossRef Medline
24. Gao, M., Wang, X., Zhang, X., Ha, T., Ma, H., Liu, L., Kalbfleisch, J. H., Gao, X., Kao, R. L., Williams, D. L., and Li, C. (2015) Attenuation of cardiac dysfunction in polymicrobial sepsis by microRNA-146a is mediated via targeting of IRAK1 and TRAF6 expression. *J. Immunol.* **195,** 672–682 CrossRef Medline
25. Ma, H., Wang, X., Ha, T., Gao, M., Liu, L., Wang, R., Yu, K., Kalbfleisch, J. H., Kao, R. L., Williams, D. L., and Li, C. (2016) MicroRNA-125b prevents cardiac dysfunction in polymicrobial sepsis by targeting TRAF6-mediated nuclear factor κB activation and p53-mediated apoptotic signaling. *J. Infect. Dis.* **214,** 1773–1783 CrossRef Medline
26. Yano, M., Kobayashi, S., Kohno, M., Doi, M., Tokuhisa, T., Okuda, S., Suetsugu, M., Hisaoka, T., Obayashi, M., Ohkusa, T., Kohno, M., and Matsuzaki, M. (2003) FKBP12.6-mediated stabilization of calcium-release channel (ryanodine receptor) as a novel therapeutic strategy against heart failure. *Circulation* **107,** 477–484 CrossRef Medline
27. Blayney, L. M., Jones, J. L., Griffiths, J., and Lai, F. A. (2010) A mechanism of ryanodine receptor modulation by FKBP12/12.6, protein kinase A, and K201. *Cardiovasc. Res.* **85,** 68–78 CrossRef Medline
28. Yano, M., Okuda, S., Oda, T., Tokuhisa, T., Tateishi, H., Mochizuki, M., Noma, T., Doi, M., Kobayashi, S., Yamamoto, T., Ikeda, Y., Ohkusa, T., Ikemoto, N., and Matsuzaki, M. (2005) Correction of defective interdomain interaction within ryanodine receptor by antioxidant is a new therapeutic strategy against heart failure. *Circulation* **112,** 3633–3643 CrossRef Medline
29. Sacherer, M., Sedej, S., Wakuła, P., Wallner, M., Vos, M. A., Kockskämper, J., Stiegler, P., Sereinigg, M., von Lewinski, D., Antoons, G., Pieske, B. M., Heinzel, F. R., and CONTICA investigators (2012) JTV519 (K201) reduces sarcoplasmic reticulum Ca^{2+} leak and improves diastolic function *in vitro* in murine and human non-failing myocardium. *Br. J. Pharmacol.* **167,** 493–504 CrossRef Medline
30. Wehrens, X. H., Lehnart, S. E., Reiken, S., van der Nagel, R., Morales, R., Sun, J., Cheng, Z., Deng, S. X., de Windt, L. J., Landry, D. W., and Marks, A. R. (2005) Enhancing calstabin binding to ryanodine receptors improves cardiac and skeletal muscle function in heart failure. *Proc. Natl. Acad Sci. U.S.A.* **102,** 9607–9612 CrossRef Medline
31. Mochizuki, M., Yano, M., Oda, T., Tateishi, H., Kobayashi, S., Yamamoto, T., Ikeda, Y., Ohkusa, T., Ikemoto, N., and Matsuzaki, M. (2007) Scavenging free radicals by low-dose carvedilol prevents redox-dependent Ca^{2+} leak via stabilization of ryanodine receptor in heart failure. *J. Am. Coll. Cardiol.* **49,** 1722–1732 CrossRef Medline
32. Okatan, E. N., Tuncay, E., and Turan, B. (2013) Cardioprotective effect of selenium via modulation of cardiac ryanodine receptor calcium release channels in diabetic rat cardiomyocytes through thioredoxin system. *J. Nutr. Biochem.* **24,** 2110–2118 CrossRef Medline
33. Oda, T., Yang, Y., Uchinoumi, H., Thomas, D. D., Chen-Izu, Y., Kato, T., Yamamoto, T., Yano, M., Cornea, R. L., and Bers, D. M. (2015) Oxidation of ryanodine receptor (RyR) and calmodulin enhance Ca release and pathologically alter, RyR structure and calmodulin affinity. *J Mol. Cell Cardiol.* **85,** 240–248 CrossRef Medline
34. Marx, S. O., Reiken, S., Hisamatsu, Y., Jayaraman, T., Burkhoff, D., Rosemblit, N., and Marks, A. R. (2000) PKA phosphorylation dissociates FKBP12.6 from the calcium release channel (ryanodine receptor): defective regulation in failing hearts. *Cell* **101,** 365–376 CrossRef Medline
35. Zalk, R., Lehnart, S. E., and Marks, A. R. (2007) Modulation of the ryanodine receptor and intracellular calcium. *Annu. Rev. Biochem.* **76,** 367–385 CrossRef Medline
36. Oda, T., Yano, M., Yamamoto, T., Tokuhisa, T., Okuda, S., Doi, M., Ohkusa, T., Ikeda, Y., Kobayashi, S., Ikemoto, N., and Matsuzaki, M. (2005) Defective regulation of interdomain interactions within the ryanodine receptor plays a key role in the pathogenesis of heart failure. *Circulation* **111,** 3400–3410 CrossRef Medline
37. Roy, J., Oger, C., Thireau, J., Roussel, J., Mercier-Touzet, O., Faure, D., Pinot, E., Farah, C., Taber, D. F., Cristol, J. P., Lee, J. C., Lacampagne, A., Galano, J. M., Durand, T., and Le Guennec, J. Y. (2015) Nonenzymatic lipid mediators, neuroprostanes, exert the antiarrhythmic properties of docosahexaenoic acid. *Free Radic. Biol. Med.* **86,** 269–278 CrossRef Medline
38. Reiken, S., Gaburjakova, M., Guatimosim, S., Gomez, A. M., D'Armiento, J., Burkhoff, D., Wang, J., Vassort, G., Lederer, W. J., and Marks, A. R. (2003) Protein kinase A phosphorylation of the cardiac calcium release channel (ryanodine receptor) in normal and failing hearts: role of phosphatases and response to isoproterenol. *J. Biol. Chem.* **278,** 444–453 CrossRef Medline
39. Zheng, J., Wenzhi, B., Miao, L., Hao, Y., Zhang, X., Yin, W., Pan, J., Yuan, Z., Song, B., and Ji, G. (2010) Ca^{2+} release induced by cADP-ribose is mediated by FKBP12.6 proteins in mouse bladder smooth muscle. *Cell Calcium* **47,** 449–457 CrossRef Medline

40. Ide, T., Tsutsui, H., Kinugawa, S., Utsumi, H., Kang, D., Hattori, N., Uchida, K., Arimura, Ki, Egashira, K., and Takeshita, A. (1999) Mitochondrial electron transport complex I is a potential source of oxygen free radicals in the failing myocardium. *Circ. Res.* **85,** 357–363 CrossRef Medline
41. Neri, M., Riezzo, I., Pomara, C., Schiavone, S., and Turillazzi, E. (2016)Oxidative-nitrosative stress and myocardial dysfunctions in sepsis: evidence from the literature and postmortem observations. *Mediators Inflamm.* **2016,** 3423450 Medline
42. Kong, X., Thimmulappa, R., Kombairaju, P., and Biswal, S. (2010) NADPH oxidase-dependent reactive oxygen species mediate amplified TLR4 signaling and sepsis-induced mortality in Nrf2-deficient mice. *J. Immunol.* **185,** 569–577 CrossRef Medline
43. Zhang, M., Zou, L., Feng, Y., Chen, Y. J., Zhou, Q., Ichinose, F., and Chao, W. (2014) Toll-like receptor 4 is essential to preserving cardiac function and survival in low-grade polymicrobial sepsis. *Anesthesiology* **121,** 1270–1280 CrossRef Medline
44. Kwon, O. S., Nelson, D. S., Barrows, K. M., O'Connell, R. M., and Drummond, M. J. (2016) Intramyocellular ceramides and skeletal muscle mitochondrial respiration are partially regulated by Toll-like receptor 4 during hindlimb unloading. *Am. J. Physiol. Regul. Integr. Comp. Physiol.* **311,** R879–R887 CrossRef Medline
45. Sepúlveda, M., Gonano, L. A., Viotti, M., Morell, M., Blanco, P., Lopez, A. M., Peroba Ramos, I., Bastos Carvalho, A., Medei, E., and Vila Petroff, M. (2017) Calcium/calmodulin protein kinase II-dependent ryanodine receptor phosphorylation mediates cardiac contractile dysfunction associated with sepsis. *Crit. Care Med.* **45,** e399–e408 CrossRef Medline
46. Yano, M., Ono, K., Ohkusa, T., Suetsugu, M., Kohno, M., Hisaoka, T., Kobayashi, S., Hisamatsu, Y., Yamamoto, T., Kohno, M., Noguchi, N., Takasawa, S., Okamoto, H., and Matsuzaki, M. (2000) Altered stoichiometry of FKBP12.6 *versus* ryanodine receptor as a cause of abnormal Ca^{2+} leak through ryanodine receptor in heart failure. *Circulation* **102,** 2131–2136 CrossRef Medline
47. Kaftan, E., Marks, A. R., and Ehrlich, B. E. (1996) Effects of rapamycin on ryanodine receptor/Ca^{2+}-release channels from cardiac muscle. *Circ. Res.* **78,** 990–997 CrossRef Medline
48. Xiao, R. P., Valdivia, H. H., Bogdanov, K., Valdivia, C., Lakatta, E. G., and Cheng, H. (1997) The immunophilin FK506-binding protein modulates Ca^{2+} release channel closure in rat heart. *J. Physiol.* **500,** 343–354 CrossRef Medline
49. Timerman, A. P., Onoue, H., Xin, H. B., Barg, S., Copello, J., Wiederrecht, G., and Fleischer, S. (1996) Selective binding of FKBP12.6 by the cardiac ryanodine receptor. *J. Biol. Chem.* **271,** 20385–20391 CrossRef Medline
50. Barg, S., Copello, J. A., and Fleischer, S. (1997) Different interactions of cardiac and skeletal muscle ryanodine receptors with FK-506 binding protein isoforms. *Am. J. Physiol.* **272,** C1726–C1733 Medline
51. Xin, H. B., Senbonmatsu, T., Cheng, D. S., Wang, Y. X., Copello, J. A., Ji, G. J., Collier, M. L., Deng, K. Y., Jeyakumar, L. H., Magnuson, M. A., Inagami, T., Kotlikoff, M. I., and Fleischer, S. (2002) Oestrogen protects FKBP12.6 null mice from cardiac hypertrophy. *Nature* **416,** 334–338 CrossRef Medline
52. Zhang, X., Tallini, Y. N., Chen, Z., Gan, L., Wei, B., Doran, R., Miao, L., Xin, H. B., Kotlikoff, M. I., and Ji, G. (2009) Dissociation of FKBP12.6 from ryanodine receptor type 2 is regulated by cyclic ADP-ribose but not β-adrenergic stimulation in mouse cardiomyocytes. *Cardiovasc. Res.* **84,** 253–262 CrossRef Medline
53. Wehrens, X. H., Lehnart, S. E., Huang, F., Vest, J. A., Reiken, S. R., Mohler, P. J., Sun, J., Guatimosim, S., Song, L. S., Rosemblit, N., D'Armiento, J. M., Napolitano, C., Memmi, M., Priori, S. G., Lederer, W. J., and Marks, A. R. (2003) FKBP12.6 deficiency and defective calcium release channel (ryanodine receptor) function linked to exercise-induced sudden cardiac death. *Cell* **113,** 829–840 CrossRef Medline
54. Zhao, Y. T., Guo, Y. B., Gu, L., Fan, X. X., Yang, H. Q., Chen, Z., Zhou, P., Yuan, Q., Ji, G. J., and Wang, S. Q. (2017) Sensitized signalling between L-type Ca^{2+} channels and ryanodine receptors in the absence or inhibition of FKBP12.6 in cardiomyocytes. *Cardiovasc. Res.* **113,** 332–342 Medline
55. Guo, T., Cornea, R. L., Huke, S., Camors, E., Yang, Y., Picht, E., Fruen, B. R., and Bers, D. M. (2010) Kinetics of FKBP12.6 binding to ryanodine receptors in permeabilized cardiac myocytes and effects on Ca sparks. *Circ. Res.* **106,** 1743–1752 CrossRef Medline
56. Efremov, R. G., Leitner, A., Aebersold, R., and Raunser, S. (2015) Architecture and conformational switch mechanism of the ryanodine receptor. *Nature* **517,** 39–43 Medline
57. Zalk, R., Clarke, O. B., des Georges, A., Grassucci, R. A., Reiken, S., Mancia, F., Hendrickson, W. A., Frank, J., and Marks, A. R. (2015) Structure of a mammalian ryanodine receptor. *Nature* **517,** 44–49 Medline
58. Yan, Z., Bai, X., Yan, C., Wu, J., Li, Z., Xie, T., Peng, W., Yin, C., Li, X., Scheres, S. H. W., Shi, Y., and Yan, N. (2015) Structure of the rabbit ryanodine receptor RyR1 at near-atomic resolution. *Nature* **517,** 50–55 Medline
59. Peng, W., Shen, H., Wu, J., Guo, W., Pan, X., Wang, R., Chen, S. R., and Yan, N. (2016) Structural basis for the gating mechanism of the type 2 ryanodine receptor RyR2. *Science* **354,** aah5324 Medline
60. Rittirsch, D., Huber-Lang, M. S., Flierl, M. A., and Ward, P. A. (2009) Immunodesign of experimental sepsis by cecal ligation and puncture. *Nat. Protoc.* **4,** 31–36 Medline
61. Deng, J., Liu, W., Wang, Y., Dong, M., Zheng, M., and Liu, J. (2012) Polydatin modulates Ca^{2+} handling, excitation-contraction coupling and β-adrenergic signaling in rat ventricular myocytes. *J. Mol. Cell Cardiol.* **53,** 646–656 CrossRef Medline
62. Zhou, Y. Y., Wang, S. Q., Zhu, W. Z., Chruscinski, A., Kobilka, B. K., Ziman, B., Wang, S., Lakatta, E. G., Cheng, H., and Xiao, R. P. (2000) Culture and adenoviral infection of adult mouse cardiac myocytes: methods for cellular genetic physiology. *Am. J. Physiol. Heart Circ Physiol.* **279,** H429–H436 Medline
63. Fauconnier, J., Meli, A. C., Thireau, J., Roberge, S., Shan, J., Sassi, Y., Reiken, S. R., Rauzier, J. M., Marchand, A., Chauvier, D., Cassan, C., Crozier, C., Bideaux, P., Lompré, A. M., Jacotot, E., *et al.* (2011) Ryanodine receptor leak mediated by caspase-8 activation leads to left ventricular injury after myocardial ischemia-reperfusion. *Proc. Natl. Acad Sci. U.S.A.* **108,** 13258–13263 CrossRef Medline
64. Yancey, D. M., Guichard, J. L., Ahmed, M. I., Zhou, L., Murphy, M. P., Johnson, M. S., Benavides, G. A., Collawn, J., Darley-Usmar, V., and Dell'Italia, L. J. (2015)Cardiomyocyte mitochondrial oxidative stress and cytoskeletal breakdown in the heart with a primary volume overload. *Am. J. Physiol. Heart Circ. Physiol.* **308,** H651–H663 CrossRef Medline